

RESEARCH

Open Access



Application of CT-based radiomics combined with laboratory tests such as AFP and PIVKA-II in preoperative prediction of pathologic grade of hepatocellular carcinoma

Meng Wu¹, Haijia Yu¹, Siwen Pang¹, Aie Liu² and Jianhua Liu^{1*}

Abstract

Background To investigate how effectively clinical features and CT-based radiomic features predict the pathological grade of hepatocellular carcinoma (HCC).

Methods We retrospectively analyzed 108 patients diagnosed with hepatocellular carcinoma who underwent pathological examination between May 2020 and May 2024 at the Second Hospital of Jilin University. All patients underwent laboratory tests and contrast-enhanced computed tomography (CECT) scanning of the liver within one month prior to pathological examination. First, we analyzed laboratory tests, such as alpha fetoprotein (AFP) and des-γ-carboxy prothrombin (PIVKA-II), to identify risk factors associated with the pathological grading of HCC. Then, we built and evaluated the performance of the clinical model. Next, we imported the arterial-phase and venous-phase images of the CECT images into the uAI Research Portal research platform for 'one-stop' processing, which included semiautomatic ROI outlining, feature extraction, dimensionality reduction, model construction and evaluation. To evaluate the model's diagnostic effectiveness, receiver operating characteristic (ROC) curves were produced, and the related accuracy, sensitivity, specificity, and area under the curve (AUC) were computed. The models were compared using the Delong test, and the clinical value of the predictive model was assessed via the use of calibration curves and decision curve analysis (DCA) to quantify the agreement between the model and the actual outcomes.

Results Poorly differentiated hepatocellular carcinoma (pHCC) is associated with risk variables such as hepatitis C virus antibodies (HCVAb), PIVKA-II, and sex. In the training and validation cohorts, the AUC values of the clinical model were 0.719 and 0.692, respectively; those of the AP model were 0.843 and 0.773; those of the VP model were 0.806 and 0.804; those of the AP + VP model were 0.953 and 0.844; and those of the AP + VP + clinical model were 0.926 (95% CI: 0.88–0.995) and 0.863 (95% CI: 0.711–1). The DCA curves revealed that the overall net benefit of the AP + VP + clinical model was greater than that of the other models and that it had the best diagnostic results.

Conclusions CT-based radiomic modeling combined with clinical features (sex) and laboratory tests (e.g., AFP and PIVKA-II) can reliably predict the pathological grade of HCC patients prior to surgery.

*Correspondence:

Jianhua Liu
jian_hua@jlu.edu.cn

Full list of author information is available at the end of the article



© The Author(s) 2025. **Open Access** This article is licensed under a Creative Commons Attribution-NonCommercial-NoDerivatives 4.0 International License, which permits any non-commercial use, sharing, distribution and reproduction in any medium or format, as long as you give appropriate credit to the original author(s) and the source, provide a link to the Creative Commons licence, and indicate if you modified the licensed material. You do not have permission under this licence to share adapted material derived from this article or parts of it. The images or other third party material in this article are included in the article's Creative Commons licence, unless indicated otherwise in a credit line to the material. If material is not included in the article's Creative Commons licence and your intended use is not permitted by statutory regulation or exceeds the permitted use, you will need to obtain permission directly from the copyright holder. To view a copy of this licence, visit <http://creativecommons.org/licenses/by-nc-nd/4.0/>.

Keywords Hepatocellular carcinoma, Pathological grade, Radiomics, AFP, PIVKA-II

Background

HCC is the sixth most common malignant tumor in the world, and it is also one of the leading causes of cancer-related death; furthermore, it accounts for 75–85% of all primary liver malignancies [1]. The degree of differentiation of HCC is an important predictor of postoperative recurrence and patient survival [2]. Furthermore, poorly differentiated HCC patients have a worse prognosis following surgical resection and a higher recurrence incidence than highly and moderately differentiated HCC patients do [3]. Preoperative prediction of the degree of differentiation of HCC will play a decisive role in the development of a patient's treatment plan, especially in patients with a high degree of differentiation; unnecessary chemotherapy can be avoided, the treatment plan of surgical resection is preferred, and good results can be achieved [4]. Although ultrasound-guided needle biopsy can identify the degree of differentiation of HCC before surgery, it is an invasive procedure with certain operational difficulties and risks and the possibility of needle metastasis [5]. Therefore, there is an urgency of need for a noninvasive test to clarify the degree of differentiation of HCC preoperatively.

Radiomics is an artificial intelligence technology that enables quantitative analysis of medical images, which overcomes the limitations of visual observation of lesions. It is a method for extracting high-throughput text features and converting them into data that can be analyzed [6]. The development of radiomic models that apply machine learning techniques can improve diagnostic accuracy and facilitate the prediction of treatment outcomes and patient prognosis. This will help to make more informed clinical decisions [7]. Radiomics has been employed in the context of HCC, including differential diagnosis, the prediction of pathological results, the evaluation of treatment efficacy and the prediction of patient prognosis [8–10]. A recent CT-based radiomic study suggested that radiomics has the potential to identify early changes in the transition from cirrhosis to HCC [11]. Huang et al. demonstrated the ability to predict the pathological grade of HCC lesions on the basis of CECT radiomics features [12].

Recent studies have demonstrated that there are a variety of markers that can be used for screening for HCC, prediction of HCC malignancy and prognosis, and may even be relevant to therapeutic strategies for HCC. Yang et al. showed that for high-risk individuals, screening for liver cancer using AFP, US, CT, and MRI is more effective than no screening at all [13]. Ma et al. showed that cystathionine-gamma-lyase may be a potential prognostic biomarker and new therapeutic target for HCC [14].

Peng et al. found a six-gene signature to be a dependable model with substantial therapeutic potential for estimating prognosis and overall survival in patients with HCC. This signature may also help doctors make decisions about the best course of treatment [15].

AFP is a commonly used clinical biomarker for the diagnosis of HCC, but it is not sensitive for the diagnosis of small HCC and early HCC. In addition, AFP is often elevated in certain benign liver diseases (e.g., chronic hepatitis and cirrhosis) [16]. The findings of several studies have indicated that serum PIVKA-II levels may represent a valuable and independent tumor marker for the diagnosis of HCC. PIVKA-II remains a valuable diagnostic tool for HCC patients whose AFP levels are below the threshold for positivity and can be employed as a supplementary diagnostic measure in conjunction with AFP [17]. PIVKA-II exhibits high sensitivity and specificity in liver tumor diagnosis, with its cutoff value remaining uninfluenced by age [18]. The combined use of these two markers significantly enhances the efficacy of diagnosing HCC. Furthermore, PIVKA-II values are linked to a range of pathological characteristics that indicate tumor invasiveness and/or a poor prognosis [17]. However, single serum biomarkers showed low sensitivity and specificity in the above studies [19].

The purpose of this study was to extract radiomic features from the arterial and venous phases of liver CECT images of patients with HCC and combine them with clinical features (age, sex) and laboratory tests such as AFP and PIVKA-II to construct a model for predicting the differentiation grade of HCC.

Methods

Patient selection

The study protocol was approved by the Ethics Committee of the Second Hospital of Jilin University (Research Review No. 114 of 2023). Given that this study was conducted in a retrospective manner, the informed consent of the enrolled patients was waived. The study recruited patients diagnosed with HCC through pathological examination at the Second Hospital of Jilin University between May 2020 and May 2024. The inclusion criteria for all the studied patients were as follows: (1) ≥ 18 years of age; (2) HCC diagnosis via pathological examination; and (3) CECT and related laboratory tests within one month prior to pathological examination. The exclusion criteria were as follows: (1) the coexistence of other malignant neoplasms; (2) the use of targeted therapy, immunotherapy or other antitumour therapy prior to pathological examination; (3) the absence of

comprehensive clinical and pathological data; and (4) suboptimal image quality and conspicuous artifacts.

Clinicopathological data

The clinical characteristics, laboratory test results and pathological data of all patients were obtained from the electronic medical records system. The demographic characteristics of the patients included age and sex, and laboratory test results included the levels of AFP, PIVKA-II, alanine aminotransferase (ALT), total bilirubin (TB), hepatitis B virus surface antigen (HBsAg), and neutrophil (NE), among other relevant parameters. To this end, we calculated and added the albumin–bilirubin (ALBI) score and inflammatory markers.

The pathological classification of HCC was based on differentiation criteria [20], and patients were divided into two groups, pHCC and nonpoorly differentiated HCC (npHCC), with the nonpoorly differentiated HCC group including moderately differentiated and highly differentiated cases. The χ^2 test and Mann–Whitney U test were used to determine whether there were significant differences between the two groups of patients with respect to categorical and continuous variables, respectively.

Clinical model construction and evaluation

Clinical features and laboratory test results with $P < 0.1$ were integrated with a logistic regression algorithm to construct a clinical model for predicting the grade of pathological differentiation of HCC. The model was

subsequently evaluated via a fivefold cross-validation method.

CT protocol

The enrolled cases were subjected to CT scans using multiple detectors, including the GE Revolution, Phillips Brilliance, Siemen Satom FORCE, and Neusoft Prime, to obtain plain, arterial, portal and delayed images. The CT scanner parameters were set as follows: tube current 250–400 mA; tube voltage 100 or 120 kVp; matrix 512 × 512; rotation time 0.25–0.60 s; and slice thickness 1.0–5.0 mm. After the acquisition of plain scan phase images, contrast medium was injected through the anterior cubital vein at a rate of 3.0 ml/second. Arterial phase, portal phase and delay phase images were obtained 25–30 s, 60 s and 150–180 s after contrast agent injection, respectively.

Image processing, feature extraction and feature selection

Figure 1 depicts our workflow through the uAI Research Portal (Shanghai United Imaging Intelligent Medical Technology Co., Ltd.) research platform for the “one-stop” radiomics workflow. First, we imported the CECT images into the uAI Research Portal. Portal, and through human–computer interaction, we performed semiautomatic layer-by-layer outlining of the ROIs on the arterial and venous phases of the CECT images to form a three-dimensional region of interest. Subsequently, radiomic features were extracted within the region of interest, including seven types of radiomic features, such as

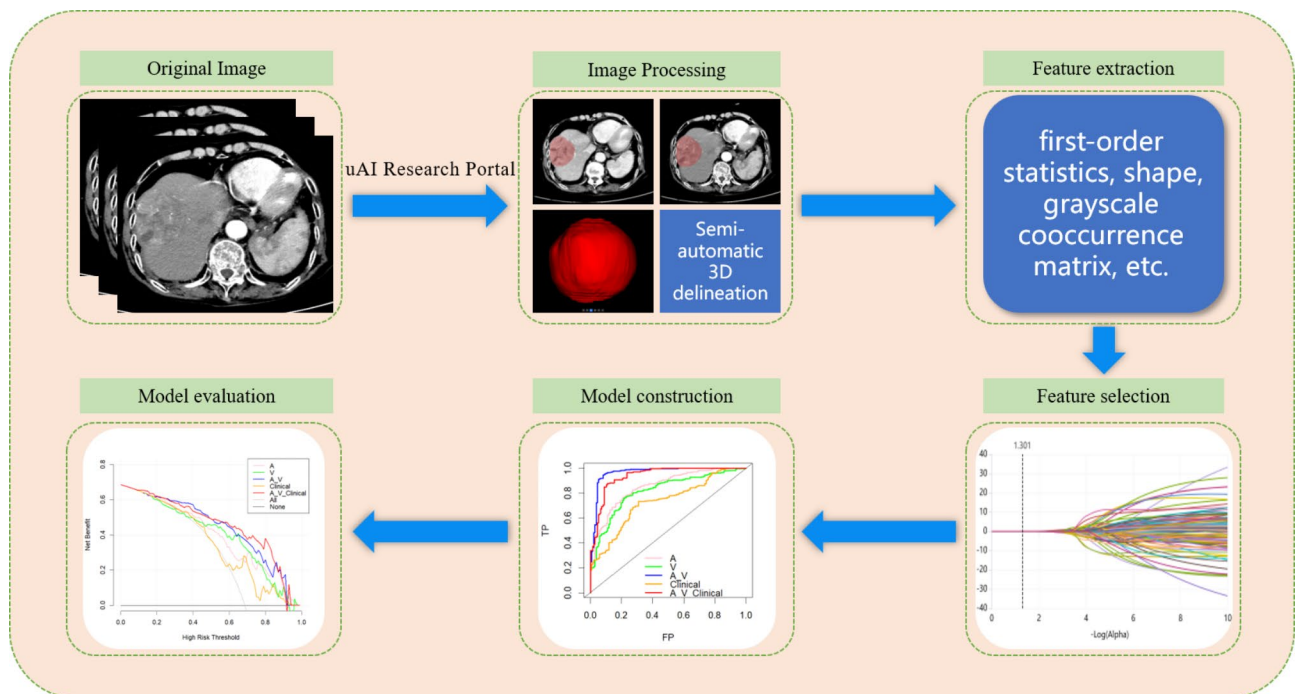


Fig. 1 Detailed flowchart including ROI segmentation, feature extraction and selection, and radiomics model construction and evaluation

first-order statistics, a gray-level covariance matrix and a gray-level dependency matrix. Next, feature extraction was performed using 25 imaging filters within the uAI research portal. Consequently, 2264 features were obtained. The platform first retains the 100 k-best features, and then, each feature is selected via least absolute shrinkage and selection operation regression (LASSO). The lasso alpha parameters for the arterial and venous phase images are 0.06 and 0.05, respectively, retaining 7 and 12 features, respectively. The features from the arterial and venous phase images were combined into 19 features, and then, through the comprehensive radiomic model of lasso ($\alpha=0.05$), 10 features were ultimately retained.

Radiomics models construction and evaluation

Models are constructed using machine learning classifiers such as logistic regression, support vector machines, and random forests. The model with the best AUC value in the validation cohort was ultimately selected, and the corresponding accuracy, sensitivity and specificity were calculated. The clinical model uses logistic regression (LR) with several parameters ($C=0.01$, penalty=l2, class weight=None, Tol=1e-05). The AP model uses LR with several parameters ($C=4.0$, penalty=l2, class weight=balanced, Tol=1e-05). The VP model uses LR with several parameters ($C=0.05$, penalty=l2, class weight=balanced, Tol=1e-05). The AP+VP model uses a support vector machine (SVM) with several parameters ($C=5.0$, Gamma=scale, Class Weight=None, Kernel=rbf). The AP+VP+Clinical model uses LR with several parameters ($C=1.5$, penalty=l2, class weight=None, Tol=1e-05). The models were subsequently compared using the DeLong test, and calibration curves and DCA were plotted to estimate the agreement between the predictive models and the actual results and to evaluate their clinical utility.

Results

Clinical characteristics

A total of 108 eligible HCC patients were enrolled in this study, 35 (32.41%) of whom were diagnosed with pHCC and 73 (67.59%) with npHCC. A comparison of the clinical characteristics of the two groups of patients revealed that factors significantly associated with the degree of differentiation of HCC included sex, PIVKA-II, and HCVAb ($P<0.05$). Among them, the number of men in the npHCC group was significantly greater than that in the pHCC group; the PIVKA-II value in the pHCC group was significantly greater than that in the npHCC group; and the number of HCVAb-positive patients in the npHCC group was significantly greater than that in the pHCC group. (Table 1).

Clinical model

We used six variables (sex, surface antigen, HCVAb, AFP, PIVKA-II, and FN) with p values less than 0.1, as shown in Table 1, to construct a clinical model for predicting the degree of pathological differentiation of hepatocellular carcinoma. The areas under the curve of the model were 0.719 (95% CI: 0.619–0.842) and 0.692 (95% CI: 0.455–0.93) for the training cohort and validation cohort, respectively, with accuracies of 0.683 and 0.629, sensitivities of 0.848 and 0.809, and specificities of 0.324 and 0.238, respectively. The clinical model clearly has some diagnostic efficacy for the pathologic differentiation of HCC, but its accuracy and specificity are poor, as shown in Table 2; Fig. 2.

Radiomics models

We selected 7 and 12 features from 4528 radiomic features (including 2264 AP features and 2264 VP features) to construct the AP model and the VP model, respectively, and then screened 10 features from 19 AP and VP features to construct the AP+VP model. The diagnostic efficacy results of all the models are presented in Table 2. Figure 2 shows the ROC curves of all the models. Among the three radiomics models, the AP+VP model has the best diagnostic performance, with AUC values of 0.953 and 0.844 in the training and validation cohorts, respectively, which are significantly greater than those of the AP model (with AUC values of 0.843 and 0.773, respectively) and the VP model (with AUC values of 0.806 and 0.804, respectively) and have the highest sensitivities (with AUC values of 0.806 and 0.804, respectively) in the training cohort and validation cohort (with AUC values of 0.969 and 0.862, respectively). In addition, the VP model had greater diagnostic efficacy in the venous phase than in the arterial phase, and the accuracy of the VP model was greater than that of the AP model in both the training cohort and the validation cohort, whereas the sensitivity of the AP model was greater than that of the VP model in both the training cohort and the validation cohort.

Combined model

Finally, we constructed an AP+VP+clinical model by combining the clinical model with the AP+VP model and obtained a model with greater diagnostic performance. The AUC values of the model in the training and validation cohorts were 0.926 (95% CI: 0.88–0.995) and 0.863 (95% CI: 0.711–1), respectively. Although the area under the curve of the AP+VP model was greater than that of the AP+VP+clinical model in the training cohort, with an area under the curve of 0.953 (95% CI: 0.917–1), the AP+VP+clinical model showed superior predictive performance in the validation cohort and was more accurate and sensitive than the AP+VP model. The specific diagnostic efficacy results for all the models are

Table 1 Baseline characteristics of HCC patients with different degrees of pathological differentiation

Variables	pHCC(n = 35)	npHCC(n = 73)	P
Age, years	60.0 (54.0–66.0)	59.0 (54.0–64.0)	0.758
Sex, n(%)			0.029
Male	24 (68.6)	63 (86.3)	
Female	11 (31.4)	10 (13.7)	
HBsAg, n(%)			0.056
Positive	30 (85.7)	50 (68.5)	
Negative	5 (14.3)	23 (31.5)	
HCVAb, n(%)			0.042
Positive	1 (2.9)	12 (16.4)	
Negative	34 (97.1)	61 (83.6)	
AFP, ng/mL	308.5 (6.0–2000.0)	10.3 (3.7–342.4)	0.068
PIVKA-II, mAU/mL	759.0 (53.2–6051.5)	173.7 (32.5–1145.4)	0.041
ALT, U/L	31.0 (25.5–42.1)	28.0 (21.0–40.0)	0.401
AST, U/L	34.0 (22.5–44.5)	30.0 (22.0–44.0)	0.434
TB, μ mol/L	17.0 (10.8–22.1)	16.0 (11.8–21.4)	0.979
DB, μ mol/L	5.9 (4.0–8.0)	4.7 (3.8–7.6)	0.66
ALB, g/L	39.4 (35.9–42.9)	40.2 (38.1–43.1)	0.442
GGT, U/L	56.0 (35.0–93.2)	50.0 (34.0–110.0)	0.634
LYM, $\times 10^9$ /L	1.3 (0.9–1.6)	1.3 (1.0–1.6)	0.549
NE, $\times 10^9$ /L	3.5 (2.7–6.6)	3.6 (3.0–4.5)	0.609
M, $\times 10^9$ /L	0.4 (0.3–0.7)	0.4 (0.3–0.5)	0.224
RDW, %	12.8 (12.3–13.5)	12.9 (12.2–13.5)	0.893
PLT, $\times 10^9$ /L	140.0 (107.0–193.5)	141.0 (108.0–190.0)	0.961
ALBI score	-32.8 (-35.6–29.6)	-33.5 (-35.9–31.7)	0.439
PLR	115.4 (87.7–160.1)	102.1 (75.5–158.3)	0.37
NLR	3.4 (2.0–5.1)	2.5 (1.7–3.7)	0.125
SII, $\times 10^9$	469.8 (254.2–860.2)	368.5 (247.2–580.8)	0.176
ANRI	9.0 (5.0–14.7)	9.2 (5.6–13.6)	0.636
ALRI	29.4 (19.9–39.0)	24.3 (13.0–41.3)	0.199
GLR	48.0 (29.1–70.5)	37.8 (25.3–80.0)	0.374
Fn	321.0 (268.0–341.5)	329.0 (298.0–389.0)	0.059
AFU	33.2 (26.8–33.2)	32.9 (27.7–33.2)	0.481

Data are reported as the medians and IQR. Clinical data with $P < 0.1$ are expressed in bold

Table 2 Predictive performance of different models

Model name	Number of features	Cohort	Accuracy	AUC (95% CI)	Sensitivity	Specificity
Clinical	6	Training	0.683	0.719(0.619–0.842)	0.324	0.848
		Validation	0.629	0.692(0.455–0.93)	0.238	0.809
AP	12	Training	0.778	0.843(0.769–0.939)	0.772	0.781
		Validation	0.703	0.773(0.584–0.973)	0.547	0.77
VP	7	Training	0.9	0.806(0.723–0.911)	0.839	0.662
		Validation	0.899	0.804(0.643–0.964)	0.795	0.674
AP + VP	10	Training	0.938	0.953(0.917–1)	0.868	0.969
		Validation	0.804	0.844(0.681–0.995)	0.676	0.862
AP + VP + Clinical	16	Training	0.877	0.926(0.88–0.995)	0.78	0.922
		Validation	0.814	0.863(0.711–1)	0.676	0.876

AP, arterial phase; VP, portal venous phase; AUC, area under the curve; CI, confidence interval. The highest value of each result in the training cohort and the validation cohort is bolded

shown in Table 2; Fig. 2. According to the DCA curves of all the models of the training cohort shown in Fig. 3A, the AP + VP + clinical model achieved better net gains in predicting the grade of HCC pathology over a larger

range of thresholds, whereas the DCA curves of all the models of the validation cohort shown in Fig. 3B indicated that the AP + VP model achieved better net gains in predicting the pathological grade of HCC over a larger

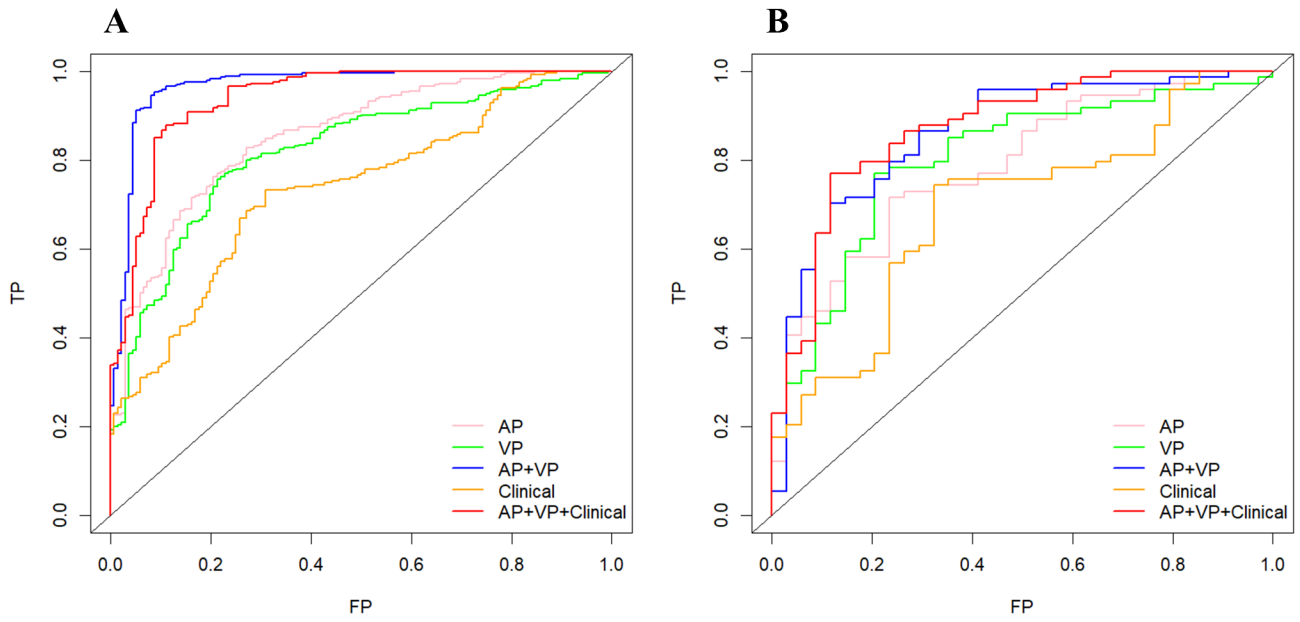


Fig. 2 ROCs of the various models. (A) Training cohort; (B) validation cohort

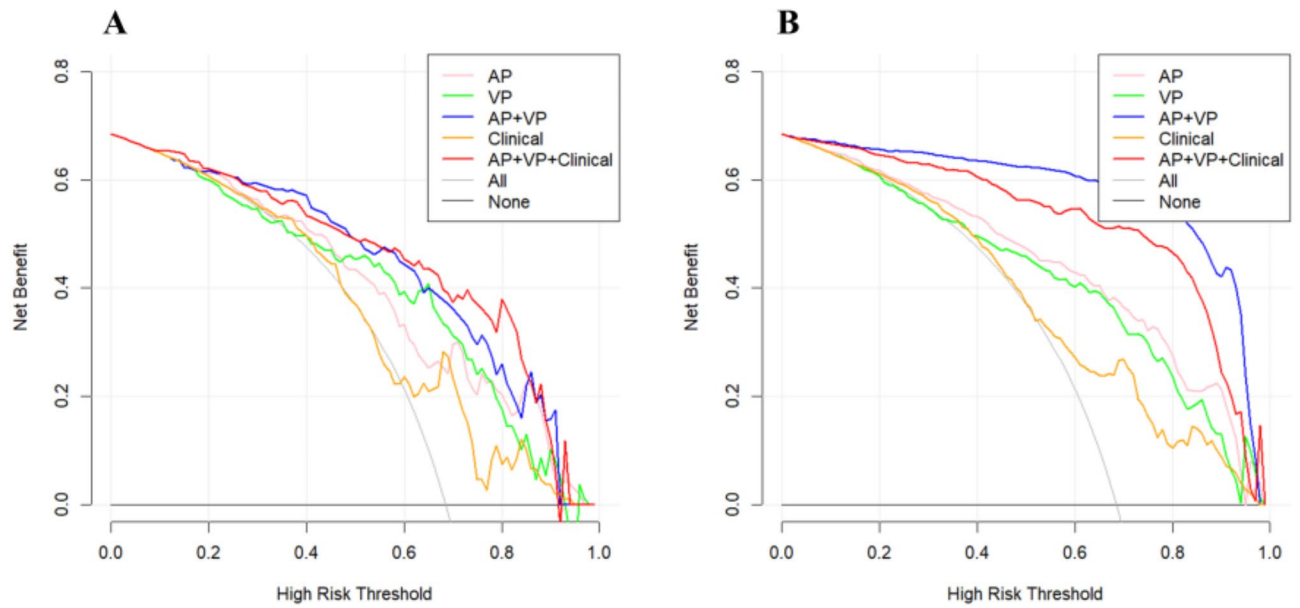


Fig. 3 Decision curves of the various models. (A) Training cohort; (B) validation cohort

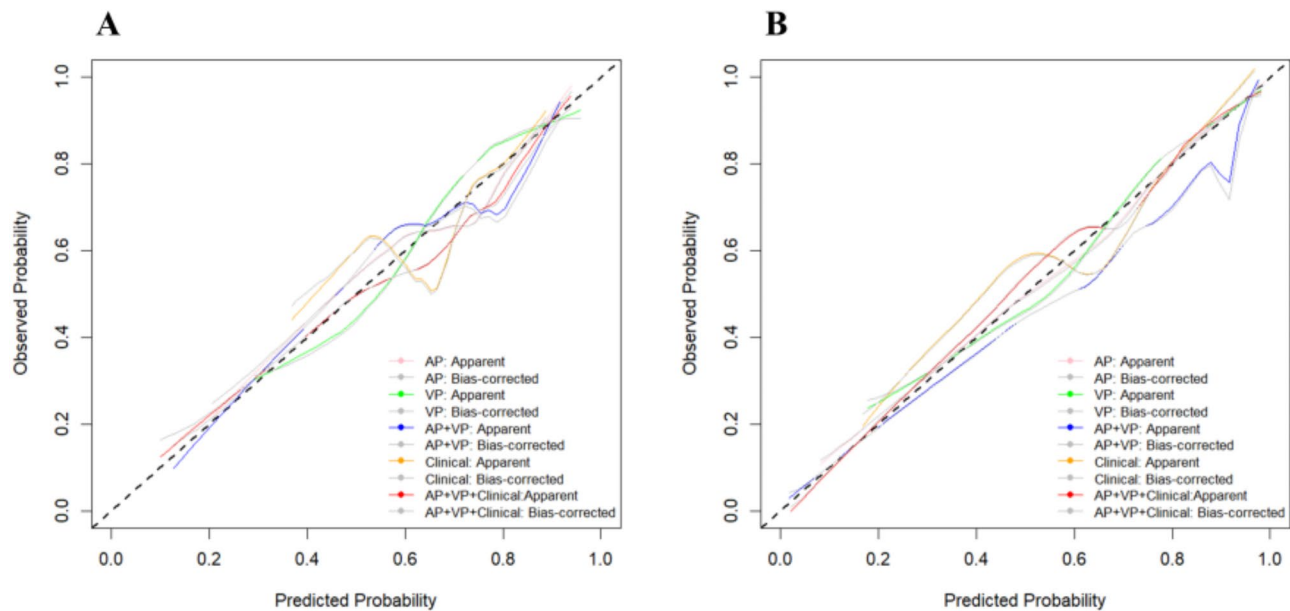


Fig. 4 Calibration curves for the various models are presented in two groups: **(A)** the training cohort and **(B)** the validation cohort

range of thresholds. There was a high degree of agreement between the predicted probabilities generated by all the radiomic models and the AP + VP + clinical model and the actual results, whereas the agreement for the clinical model was relatively poor. As shown in Fig. 4.

Discussion

Guidelines published in the journal *Liver Cancer* in 2020 suggest that although survival rates for patients with HCC treated with radical therapy have improved significantly, the overall 5-year survival for patients with HCC remains dismal and may be related to the fact that the majority of patients with HCC are able to receive only localized or systemic antitumor therapy after their initial diagnosis [21]. The presence of pathological differentiation is an important prognostic indicator in patients with HCC [22]. The clinical treatment options for HCC differ across stages and degrees of differentiation [23]. It is therefore imperative that an accurate prediction of the pathological grade of HCC be made prior to surgery, as this will inform clinical decisions and the prescription of the most appropriate individualized treatment.

This study developed and validated a noninvasive method for predicting the pathologic differentiation of HCC. We combined clinical characteristics (sex), laboratory test results (including AFP, PIVKA-II, and HBsAg), and CECT data to construct an AP + VP + clinical model for predicting the pathological grade of HCC. The results of the present study demonstrated that the fusion model

had the best predictive performance, with an AUC value of 0.863 (95% CI: 0.711–1) in the validation cohort, and achieved greater net benefits. The results of the calibration and decision curve analyses further confirmed the robustness and clinical applicability of the model.

The application of machine learning algorithms and statistical analysis to radiomic features allows the development of predictive models capable of extracting radiomic features at the microscopic level. Radiomics models are able to distinguish HCC from other liver lesions, assess tumor status, predict treatment efficacy, and even predict patient prognosis [24]. In a study by Liu et al., an MRI-based radiomic model was constructed. The AUCs of eight classifiers for diagnosing pHCC were between 0.85 and 1.00 in the training cohort and between 0.73 and 0.88 in the validation cohort [25]. Han et al. included 137 patients to construct an MRI-based radiomic model. The hepatobiliary phase model demonstrated the most promising results, with an AUC of 0.80 ± 0.09 in the internal validation phase and 0.70 ± 0.09 in the external validation phase [26]. A CT-based radiomics model was constructed by Huang et al. to predict the pathological grade of hepatocellular carcinoma. The radiomics model derived from both the arterial and venous phases showed the best diagnostic performance, with an AUC of 0.842 in the validation cohort. However, the AUC value for a clinical model developed using AFP, NEU, and HBsAg was less than optimal. The researchers therefore chose to abandon the model [12].

In our study, the CT-based radiomic model demonstrated a superior AUC and accuracy compared with those of previous studies, indicating its efficacy in predicting HCC differentiation. The aforementioned findings may be attributed to the considerable number of quantitative radiomic features extracted from the CECT images ($n = 4528$). A number of techniques, including LASSO, were subsequently employed to identify the most robust features, which were then used to develop the radiomic model. This process may have contributed to the higher AUC. The ROC curve of the AP + VP model also revealed excellent diagnostic efficacy in our radiomics models, with AUC values of 0.953 (95% CI: 0.917–1) and 0.844 (95% CI: 0.681–0.995) for the training cohort and validation cohort, respectively.

Viral hepatitis (viral hepatitis B and viral hepatitis C) is the main cause of hepatocellular carcinoma in China, and whether this is related to the degree of differentiation of hepatocellular carcinoma needs to be investigated. AFP is a conventional biomarker for the surveillance of HCC. However, its sensitivity is insufficient for this purpose [27]. Zhou et al. demonstrated that the positivity rate of PIVKA-II prior to resectable HCC surgery was markedly higher than that of AFP [28]. In recent years, PIVKA-II has become a routine clinical test. To more accurately predict the pathologic differentiation of HCC, scholars have developed many nomogram models to identify more accurate biomarkers. A study by Zhou et al. demonstrated that preoperative laboratory tests, including ALRI, AFP, PIVKA-II, HBsAg, and HCVAb, were associated with poor tumor differentiation. Among these factors, AFP, PIVKA-II and HCVAb were identified as independent predictors of the degree of pathological differentiation of HCC [29]. The results of our study revealed that PIVKA-II and HCVAb were significantly correlated with the degree of pathological differentiation of HCC ($P < 0.05$). However, the conclusion that HBsAg ($P = 0.056$) and AFP ($P = 0.068$) were significantly correlated was not supported by the results of this study.

Inflammation is widely accepted as one of the most significant characteristics of cancer [30], and it has been demonstrated that HCC is an inflammatory cancer [31]. Luo et al. proposed that the NLR is an independent prognostic factor for HCC and a reliable biomarker for predicting the overall survival rate of patients with HCC [22]. Wang et al. demonstrated the independent predictive capacity of inflammatory biomarkers, including the NLR and ALRI, with respect to the pathological grade of HCC [32]. Nevertheless, our study, which involved seven inflammatory markers (NLR, PLR, and ALRI), revealed that all the inflammatory indicators were not significantly different. This outcome may be attributable to the relatively limited sample size employed.

Our study has several limitations. First, all the CT image data were obtained from a single center, and this was a retrospective study. The CT images used in our study were from different scanning instruments, and imaging from different instruments may have had some impact on the results of feature extraction; therefore, whether the model can work prospectively is still an open question. Therefore, in our next research plan, we will conduct a multicenter prospective study using the same CT scanning instrument to further explore the diagnostic potential of radiomics-based modeling. Second, our study focused on the relationship between high-throughput imaging features extracted from tumor ROIs and pathologic stage. To quantify tumor heterogeneity more comprehensively, more attention needs to be given to peritumor information, combined with more clinico-pathological information, to build more accurate individualized disease assessment models. Therefore, in the future, we need to optimize our model on the basis of the above limitations and conduct prospective studies, which may help improve the diagnostic performance of imaging histology models for the degree of pathological differentiation of HCC. Third, it has been shown that tumor-associated lymphatic vessel density is a reliable biomarker of tumor prognosis after radical tumor resection [33], and this marker may be considered for inclusion in our future studies related to postoperative prognosis of hepatocellular carcinoma.

Conclusion

In conclusion, our radiomics analysis of HCC patients by CECT images suggests that extraction of arterial and venous phase features may be a method for preoperative prediction of HCC pathologic differentiation. In addition, the combination of clinical features and laboratory findings (e.g., alpha-fetoprotein and PIVKA-II) may improve the diagnostic efficacy of the radiomics model and provide a new noninvasive method for predicting the degree of differentiation of HCC and for clinical decision making.

Abbreviations

HCC	Hepatocellular carcinoma
CECT	Contrast-enhanced computed tomography
AFP	Alpha fetoprotein
PIVKA-II	des- γ -carboxy prothrombin
ROC	Receiver operating characteristic
AUC	Area under the curve
DCA	Decision curve analysis
ALT	Alanine aminotransferase
AST	Aspartate aminotransferase
TB	Total bilirubin
DB	Direct bilirubin
GGT	γ -glutamyl transferase
ALB	Albumin
HBsAg	Hepatitis B virus surface antigen
HCVAb	Hepatitis C virus antibodies
RDW	Red blood cell distribution width

NE	Neutrophil
LYM	Lymphocyte
M	Monocyte
PLT	Platelet
Fn	Fibronectin
AUF	α -L-fucosidase
PLR	Platelet to lymphocyte ratio
NLR	Neutrophil to lymphocyte ratio
SII	Systemic immune-inflammation index
ANRI	Aspartate aminotransferase to neutrophil ratio index
ALRI	Aspartate aminotransferase to lymphocyte ratio index
GLR	γ -glutamyl transferase to lymphocyte ratio
ALBI	Albumin-bilirubin
pHCC	Poorly differentiated hepatocellular carcinoma
npHCC	non-poorly differentiated HCC
LASSO	Least Absolute Shrinkage and Selection Operation Regression

Acknowledgements

First of all, we are especially grateful to all the patients and their families who participated in this study. We thank all the team members of the Department of Radiology and Department of Pathology at the Second Hospital of Jilin University and Shanghai United Imaging Intelligence Co., Ltd.

Author contributions

M.W conceived the study and wrote the draft. HJ.Y and SW.P extracted data from clinical charts, elaborated the data set and analyzed the data. A.E.L was responsible for the radiomics processing. J.H.L revised the article. All authors approved the final version of the article.

Funding

The Program of Youth Science and Technology Innovation and Entrepreneurship Outstanding Talents (Team) of Jilin Province, China (No. 20230508063RC); the Excellent Youth Training Foundation of Jilin University, China (No. 419080520665); and the Innovation and Entrepreneurship Talent Funding Program of Jilin Province, China.

Data availability

The datasets used and/or analyzed in the current study are available from the corresponding author upon reasonable request.

Declarations

Ethics approval and consent to participate

All methods used in this study were conducted in accordance with the Declaration of Helsinki and approved by the local institutional review board (Ethics Committee of the Second Hospital of Jilin University). Informed consent was waived for this retrospective study.

Consent for publication

NA.

Competing interests

The authors declare no competing interests.

Author details

¹Department of Radiology, The Second Hospital of Jilin University, Changchun, China

²Department of Research and Development, Shanghai United Imaging Intelligence Co., Ltd, Shanghai, China

Received: 3 November 2024 / Accepted: 10 February 2025

Published online: 17 February 2025

References

- Sung H, Ferlay J, Siegel RL, Laversanne M, Soerjomataram I, Jemal A, Bray F. Global cancer statistics 2020: GLOBOCAN estimates of incidence and mortality worldwide for 36 cancers in 185 countries. *Ca-a Cancer J Clin.* 2021;71(3):209–49.
- Shinkawa H, Tanaka S, Kabata D, Takemura S, Amano R, Kimura K, Kinoshita M, Kubo S. The prognostic impact of Tumor differentiation on recurrence and survival after resection of Hepatocellular Carcinoma is dependent on Tumor size. *Liver Cancer.* 2021;10(5):461–72.
- Zhou L, Rui JA, Zhou WX, Wang SB, Chen SG, Qu Q. Edmondson-Steiner grade: a crucial predictor of recurrence and survival in hepatocellular carcinoma without microvascular invasion. *Pathol Res Pract.* 2017;213(7):824–30.
- Lin SH, Eng HL, Liu YW, Lin CC, Yong CC, Wang CC, Chen CL, Kuo FY, Cheng YF, Wang JH, et al. Characteristics and prognosis of patients with large well-differentiated hepatocellular carcinoma who have undergone resection. *Am J Surg.* 2022;223(2):339–45.
- Vernuccio F, Rosenberg MD, Meyer M, Choudhury KR, Nelson RC, Marin D. Negative biopsy of focal hepatic lesions: decision Tree Model for Patient Management. *AJR Am J Roentgenol.* 2019;212(3):677–85.
- Miranda Magalhaes Santos JM, Clemente Oliveira B, Araujo-Filho JAB, Assuncao-Jr AN, de Carlos Tavares Rocha MMFA, Horvat C, Menezes JV, Horvat MR. State-of-the-art in radiomics of hepatocellular carcinoma: a review of basic principles, applications, and limitations. *Abdom Radiol (NY).* 2020;45(2):342–53.
- Gillies RJ, Kinahan PE, Hricak H. Radiomics: images are more than pictures, they are data. *Radiology.* 2016;278(2):563–77.
- Wu J, Liu A, Cui J, Chen A, Song Q, Xie L. Radiomics-based classification of hepatocellular carcinoma and hepatic haemangioma on precontrast magnetic resonance images. *BMC Med Imaging.* 2019;19(1):23.
- Hu X, Li C, Wang Q, Wu X, Chen Z, Xia F, Cai P, Zhang L, Fan Y, Ma K. Development and External Validation of a Radiomics Model Derived from Preoperative Gadoteric Acid-enhanced MRI for Predicting histopathologic Grade of Hepatocellular Carcinoma. *Diagnostics (Basel)* 2023, 13(3).
- Shan QY, Hu HT, Feng ST, Peng ZP, Chen SL, Zhou Q, Li X, Xie XY, Lu MD, Wang W, et al. CT-based peritumoral radiomics signatures to predict early recurrence in hepatocellular carcinoma after curative tumor resection or ablation. *Cancer Imaging.* 2019;19(1):11.
- Guo L, Hao X, Chen L, Qian Y, Wang C, Liu X, Fan X, Jiang G, Zheng D, Gao P, et al. Early warning of hepatocellular carcinoma in cirrhotic patients by three-phase CT-based deep learning radiomics model: a retrospective, multicentre, cohort study. *EClinicalMedicine.* 2024;74:102718.
- Huang Y, Chen L, Ding Q, Zhang H, Zhong Y, Zhang X, Weng S. CT-based radiomics for predicting pathological grade in hepatocellular carcinoma. *Front Oncol.* 2024;14:1295575.
- Yang J, Yang Z, Zeng X, Yu S, Gao L, Jiang Y, Sun F. Benefits and harms of screening for hepatocellular carcinoma in high-risk populations: systematic review and meta-analysis. *J Natl Cancer Cent.* 2023;3(3):175–85.
- Ma Y, Wang S, Ding H. Bioinformatics analysis and experimental validation of cystathionine-gamma-lyase as a potential prognosis biomarker in hepatocellular carcinoma. *Biocell.* 2024;48(3):463–71.
- Peng B, Ge Y, Yin G. A novel prognostic gene signature, nomogram and immune landscape based on tanshinone IIA drug targets for hepatocellular carcinoma: Comprehensive bioinformatics analysis and in vitro experiments. *Biocell.* 2023;47(7):1519–35.
- Choi JY, Jung SW, Kim HY, Kim M, Kim Y, Kim DG, Oh EJ. Diagnostic value of AFP-L3 and PIVKA-II in hepatocellular carcinoma according to total-AFP. *World J Gastroenterol.* 2013;19(3):339–46.
- Feng H, Li B, Li Z, Wei Q, Ren L. PIVKA-II serves as a potential biomarker that complements AFP for the diagnosis of hepatocellular carcinoma. *BMC Cancer.* 2021;21(1):401.
- Gao H, Xie C, Wang J, Ma J, Liu S, Xie L, Zheng Y, Dong R, Wang S, Fang Y, et al. PIVKA-II combined with alpha-fetoprotein for the diagnostic value of hepatic tumors in children: a multicenter, prospective observational study. *Hepatol Int.* 2024;18(4):1326–35.
- Wang Z, Qin H, Liu S, Sheng J, Zhang X. Precision diagnosis of hepatocellular carcinoma. *Chin Med J (Engl).* 2023;136(10):1155–65.
- Loy LM, Low HM, Choi JY, Rhee H, Wong CF, Tan CH. Variant Hepatocellular Carcinoma subtypes according to the 2019 WHO classification: an imaging-focused review. *AJR Am J Roentgenol.* 2022;219(2):212–23.
- Zhou J, Sun H, Wang Z, Cong W, Wang J, Zeng M, Zhou W, Bie P, Liu L, Wen T, et al. Guidelines for the diagnosis and Treatment of Hepatocellular Carcinoma (2019 Edition). *Liver Cancer.* 2020;9(6):682–720.
- Luo H, Huang C, Meng M, Zhang M, Li Z, Huang J. Combination of neutrophil/lymphocyte ratio and albumin/bilirubin grade as a prognostic predictor for hepatocellular carcinoma patients undergoing curative hepatectomy. *BMC Gastroenterol.* 2023;23(1):162.

23. Kawano Y, Kaneya Y, Aoki Y, Yoshioka M, Matsushita A, Shimizu T, Ueda J, Takata H, Taniai N, Kanda T, et al. Medical Treatment for Hepatocellular Carcinoma in Japan. *J Nippon Med Sch*. 2022;89(2):154–60.
24. Castaldo A, De Lucia DR, Pontillo G, Gatti M, Cocozza S, Ugga L, Cuocolo R. State of the art in Artificial Intelligence and Radiomics in Hepatocellular Carcinoma. *Diagnostics (Basel)* 2021, 11(7).
25. Liu HF, Lu Y, Wang Q, Lu YJ, Xing W. Machine learning-based CEMRI radiomics integrating LI-RADS features achieves optimal evaluation of Hepatocellular Carcinoma differentiation. *J Hepatocell Carcinoma*. 2023;10:2103–15.
26. Han YE, Cho Y, Kim MJ, Park BJ, Sung DJ, Han NY, Sim KC, Park YS, Park BN. Hepatocellular carcinoma pathologic grade prediction using radiomics and machine learning models of gadoteric acid-enhanced MRI: a two-center study. *Abdom Radiol (NY)*. 2023;48(1):244–56.
27. Tayob N, Kanwal F, Alsarraj A, Hernaez R, El-Serag HB. The performance of AFP, AFP-3, DCP as Biomarkers for Detection of Hepatocellular Carcinoma (HCC): a phase 3 Biomarker Study in the United States. *Clin Gastroenterol Hepatol*. 2023;21(2):415–e423414.
28. Zhou Z, Liu J, Xu X. A commentary on 'Prothrombin induced by vitamin K Absence-II versus alpha-fetoprotein in detection of both resectable hepatocellular carcinoma and early recurrence after curative liver resection: a retrospective cohort study' (*Int J Surg* 2022;105:106843). *Int J Surg* 2023, 109(11):3656–3658.
29. Zhou Z, Cao S, Chen C, Chen J, Xu X, Liu Y, Liu Q, Wang K, Han B, Yin Y. A Novel Nomogram for the preoperative prediction of Edmondson-Steiner Grade III-IV in Hepatocellular Carcinoma patients. *J Hepatocell Carcinoma*. 2023;10:1399–409.
30. Hanahan D, Weinberg RA. Hallmarks of cancer: the next generation. *Cell*. 2011;144(5):646–74.
31. Xue TC, Jia QA, Ge NL, Zhang BH, Wang YH, Ren ZG, Ye SL. The platelet-to-lymphocyte ratio predicts poor survival in patients with huge hepatocellular carcinoma that received transarterial chemoembolization. *Tumour Biol*. 2015;36(8):6045–51.
32. Wang F, Qin Y, Wang ZM, Yan CY, He Y, Liu D, Wen L, Zhang D. A dynamic online Nomogram based on Gd-EOB-DTPA-Enhanced MRI and inflammatory biomarkers for preoperative prediction of pathological Grade and Stratification in Solitary Hepatocellular Carcinoma: a Multicenter Study. *Acad Radiol*. 2024;31(10):4021–33.
33. Li J, Wang Q-B, Liang Y-B, Chen X-M, Luo W-L, Li Y-K, Chen X, Lu Q-Y, Ke Y. Tumor-associated lymphatic vessel density is a reliable biomarker for prognosis of esophageal cancer after radical resection: a systemic review and meta-analysis. *Front Immunol* 2024, 15.

Publisher's note

Springer Nature remains neutral with regard to jurisdictional claims in published maps and institutional affiliations.